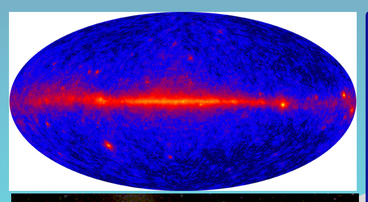

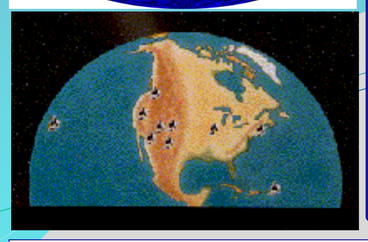

Connection between γ-ray Activity, Emission Line Variability, and Jet Behavior in Blazars

S.G. Jorstad[1,2], A.P. Marscher[1], V.M. Larionov[2], K.E. Williamson[1], Z.R. Weaver[1], and M.A. Gurwell[3]

[1]Boston University; [2]St. Petersburg State Univ., Russian Federation; [3] Center for Astrophysics

BOSTON UNIVERSITY

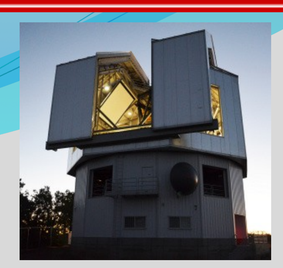

Abstract: We analyze total and polarized intensity images obtained with the Very Long Baseline Array (VLBA) at 43 GHz of the quasar CTA102 during a dramatic γ-ray/multi-wavelength outburst in 2016-2017 December, and of the quasar 4C+29.45 (1156+295, Ton 599) during a VHE event at the end of 2017. Using the 4.3 m Discovery Channel Telescope (DCT) of Lowell Observatory, we have also monitored MgII, FeII, and FIII emission lines of these quasars during the outbursts. In both cases a significant increase of the total and polarized flux in the mm-wave VLBI core contemporaneous with the high-energy events was observed, along with the appearance of superluminal knots in the jets. 10 years of VLBA monitoring of the quasars reveals the existence of quasi-stationary features in the inner parsec-scale jet in addition to the VLBI core. Based on the kinematics of the superluminal knots and position of the quasi-stationary features, we connect the structure of the γ-ray events with propagation of superluminal knots through the core and stationary features. Analysis of properties of the emission lines shows correlated variability between the flux of the FeII and FeIII emission lines, optical continuum, and γ-ray flux, which suggests that the jet plays a role in the emission line excitation. We discuss the properties and nature of the enhanced γ-ray emission, emission line variability, and jet behavior.

Multi-Wavelength Light Curves of the Quasars 4C+29.45 and CTA102 over 10 yr and Jet Behavior during the Dramatic Outbursts in 2016-2017 (CTA102) and 2017-2018 (4C+29.45)

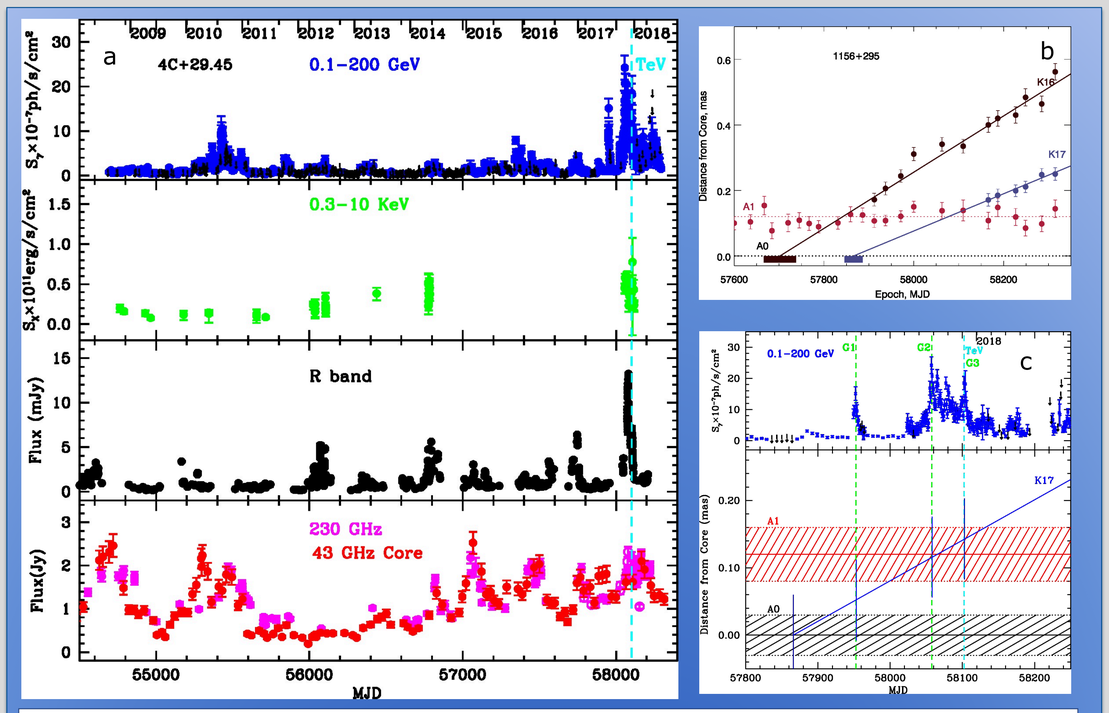

Fig. 1. a) MW light curves of 4C+29.45 from 2008 August to 2018 July; from top: 1) γ-ray flux at 0.1-200 GeV; 2) X-ray flux at 0.3-10 keV; 3) Optical flux density in R band at λ_{eff} =6580Å; 4) Radio flux densities at 230 GHz (magenta) and in 43 GHz VLBI core (red), dashed cyan line shows the time of the detection at E>100 GeV by MAGIC and VERITAS (Atel##11061, 11075). b) Separation from the VLBI core, A0 (black dotted line), of quasi-stationary feature A1 (red), and superluminal knots K16 (brown) and K17 (blue); red dotted line indicates the average position of A1, brown and blue lines represent ballistic motion of K16 and K17, respectively, with uncertainties in their ejection time from the core shown on the A0 line; Fig. 2 shows positions of knots in 43 GHz images according to modelling. c) top: γ-ray light curve during the 2017-2018 outburst with the highest γ-ray peaks indicated by green dashed lines as G1, G2, G3, and TeV; solid black line marks the position of the core, with the average size of the core during the outburst shown by the black shaded area; the red solid line and red shaded area are the same as for feature A1; the blue diagonal line shows motion of K17 with blue vertical lines marking the position of K17 during the highest γ-ray peaks, while the length of these lines corresponds to the size of K17 when it first appeared in the jet.

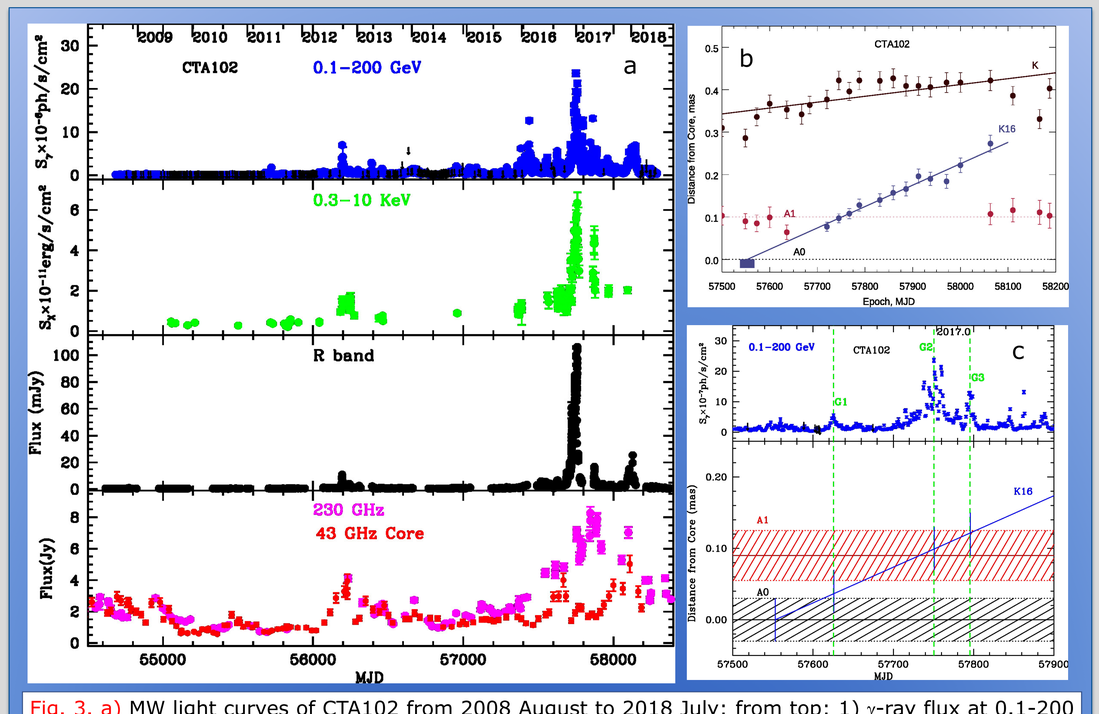

Fig. 3. a) MW light curves of CTA102 from 2008 August to 2018 July: from top: 1) γ-ray flux at 0.1-200 GeV; 2) X-ray flux at 0.3-10 keV; 3) Optical flux density in R band at λ_{eff} =6580Å; 4) Radio flux densities at 230 GHz (magenta) and in 43 GHz VLBI core (red). b) Separation from the VLBI core, A0 (black dotted line), of the quasi-stationary feature A1 (red), and superluminal knots K (brown) and K16 (blue); red dotted line indicates the average position of A1, blue solid line represents ballistic motion of K16, with uncertainty of the ejection time from the core shown on the A0 line; Fig. 4 shows positions of K16 at 43 GHz images according to modelling. c) top: γ-ray light curve during the 2016 outburst with the highest γ-ray peaks indicated by green dashed lines as G1, G2, and G3; bottom: solid black line marks the position of the core, with the average size of the core during the outburst shown by the black shaded area; the red solid line and red shaded area are the same for feature A1; the blue diagonal line shows motion of K16 with blue vertical lines marking the position of K16 during the highest γ-ray peaks, while the length of these lines corresponds to the size of K16 when it first appeared in the jet.

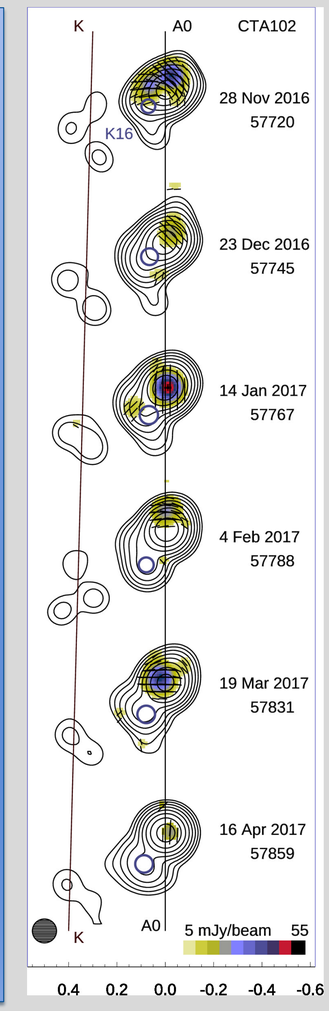

Fig. 4 (far right). VLBA total (contours) and polarized (color scale) intensity images at 43 GHz of the quasar CTA102, with a total intensity peak of 2390 mJy/beam and contour levels starting at 0.4% of the peak and increasing by factors of 2; the images are convolved with a circular beam of 0.1x0.1 mas; black line segments within images show direction of linear polarization, blue circles indicate position and size of knot K16 according to modelling.

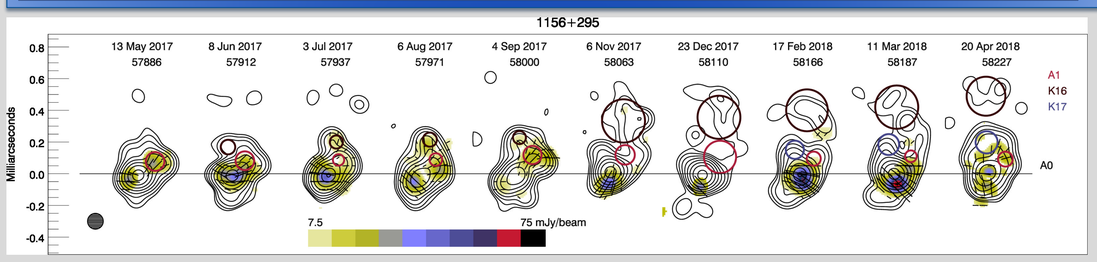

Fig. 2. VLBA total (contours) and polarized (color scale) intensity images at 43 GHz of the quasar 4C+29.45 (1156+295), with a total intensity peak of 2300 mJy/beam and contour levels starting at 0.5% of the peak and increasing by factors of 2; the images are convolved with a circular beam of 0.1x0.1 mas corresponding to the resolution of the longest baselines; black line segments within images show direction of linear polarization, while circles indicate position and size of knots A1 (red), K16 (brown), and K17 (blue) according to modelling.

Optical Spectra of CTA102, z=1.037

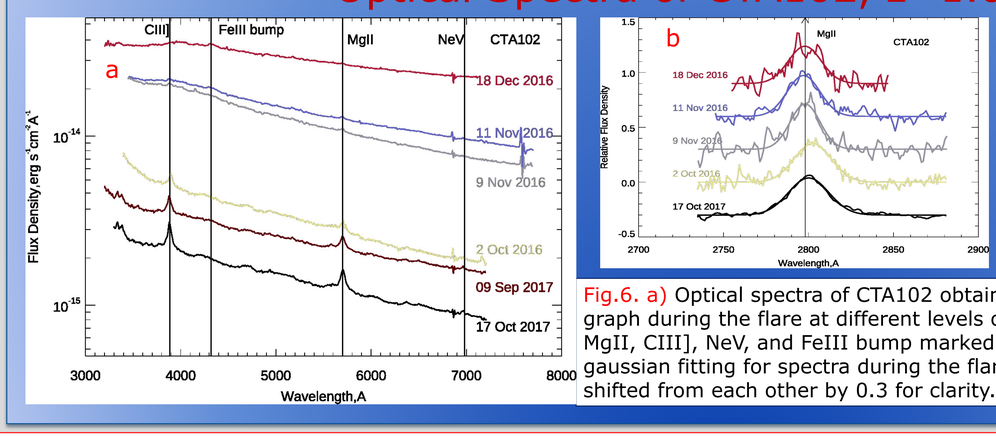

Fig.6. a) Optical spectra of CTA102 obtained at the DCT with the DeVeny spectrograph during the flare at different levels of optical flux, with emission features, MgII, CIII], NeV, and FeIII bump marked. b) Profiles of MgII line and their gaussian fitting for spectra during the flare, with continuum subtracted; lines are shifted from each other by 0.3 for clarity. c) The same as in Fig. 6b for FeIII bump.

Optical Spectra of 4C+29.45, z=0.729

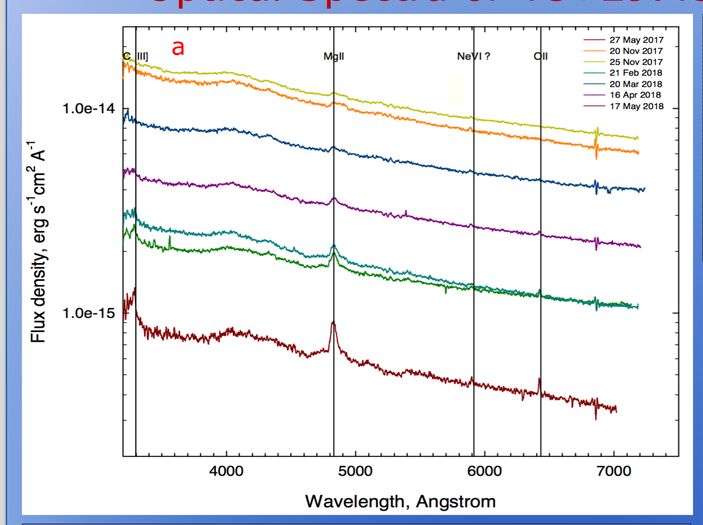

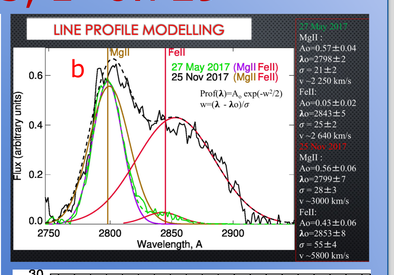

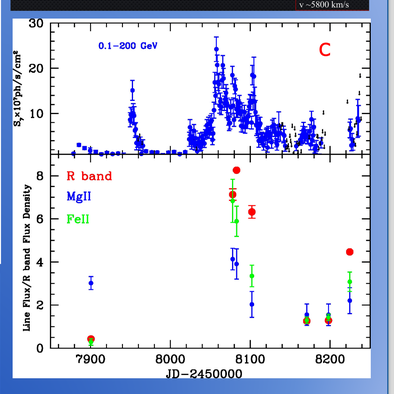

Fig.5. a) Optical spectra of 4C+29.45 obtained at the DCT with the DeVeny spectrograph during the flare at different levels of optical flux with emission spectral features, MgII, CIII], and OII marked. MgII line has an increasing red wing as the optical flux rises, which we attribute to an increase in flux of FeII complex as shown in line profile modelling in panel b; c) top - γ-ray light curve; bottom – R band flux density in mJy (red), Mg II (blue), and FeII (green) flux (in 10^{-15} erg/cm^2/s) vs. time.

Summary. The dramatic MW outbursts of the quasars 4C+29.45 in 2017-2018 and CTA102 in 2016 -2017 were a culmination of γ-ray activity that began in each source a year earlier, also apparent at millimeter wavelengths. The outbursts possess a number of important characteristics, which are similar for both sources:

I. The structure of the main part of each outburst (Figs. 1a & 3a) is similar at γ-ray, X-ray, and optical wavelengths, with peaks at different wavelengths occurring simultaneously within uncertainties of sampling. (There is a highly significant correlation between the γ-ray and R band optical light curves with zero delay.)

II. There is a striking apparent relationship between the structure of the main part of the γ-ray outburst and jet behavior presented in Figs. 1c & 3c for 4C+29.45 and CTA102, respectively:
1). The enhanced γ-ray activity starts as K17 (4C+29.45) / K16 (CTA102) passes through the VLBI core, A0, with the first peak of γ-ray flux, G1, occurring when the knot exits the core; 2). The most prominent γ-ray activity, peaks G2 & G3 (+ TeV peak in 4C+29.45), is observed as the knot crosses the quasi-stationary feature, A1; and 3). The violent γ-ray activity finishes as the knot leaves A1. The presence of quasi-stationary feature A1 has been observed previously in both jets (Jorstad et al. 2017, ApJ, 846, 98).

III. An association of the passage of a superluminal knot through A1 with the 2012 γ-ray outburst in CTA102 was reported by Casadio et al. (2015, ApJ, 813, 51), while the γ-ray outburst of 4C+29.45 in 2010 was attributed to propagation of several superluminal knots through the innermost parsec-scale region of the quasar (Ramakrishnan et al. 2014, MNRAS, 445, 1636).

IV. The flux of the MgII and, especially, FeII emission lines increases with the continuum on a days-weeks timescale in 4C+29.5 (Fig. 5), as observed in 3C454.3 (León-Tavares et al. 2013, ApJL, 763, L36), implying jet involvement in the line ionization. In CTA102 flux of MgII line is almost stable (Fig. 6b), although flux of FIII bump rises with the continuum (Fig. 6c), implying different regions for the emission line production as suggested by Baldwin et al. (2004, ApJ, 615,610) who found also that microturbulence is needed to excite Fe emission features.

The research at Boston University is supported by NASA Fermi GI grant 80NSSC17K0649 and NSF grant AST-1615796. The St.Petersburg University group acknowledges support from Russian Science Foundation grant 17-12-01029.